Microfabrication and testing of suspended structures compatible with silicon-on-insulator technology

A. A. Ayón,[a] K. Ishihara, R. A. Braff, H. H. Sawin, and M. A. Schmidt
Microsystems Technology Laboratories, Massachusetts Institute of Technology, Cambridge, Massachusetts 02139

(Received 16 February 1999; accepted 21 May 1999)

The footing or notching effect arises during the dry overetching of silicon layers on top of dielectric films. The visible consequence of this effect is the resulting etch that propagates along the interface between the underlying dielectric films and the silicon layer. Footing is usually considered an undesirable artifact during etching. Thus, the vast majority of efforts made to date have been oriented towards reducing or eliminating the aforementioned effect. There is, however, another alternative that has not been fully exploited: the application of the notching effect in the microfabrication of released structures. Furthermore, with deep reactive ion etching (DRIE) tools it is also feasible to deposit fluorocarbon films for electrical isolation purposes *in situ*. Thus, it is possible to microfabricate suspended structures by combining the footing effect with the capabilities offered by DRIE. For this purpose, we have developed, built, and tested suspended electrostatic actuators applying this new microfabrication scheme. The process is well suited for applications involving silicon-on-insulator wafers. Electrostatic actuators microfabricated with this passivation film subsequently underwent 10^5 pull-in cycles without failure. © *1999 American Vacuum Society*. [S0734-211X(99)07904-4]

I. INTRODUCTION

The footing or notching effect, which arises due to the differential charging of sidewalls and bottom of features, is observed when overetching polysilicon or single crystal silicon layers on top of dielectric films[1] (see Fig. 1). This effect is usually negligible in conventional reactive ion etching (RIE) of submicron features due to the low current fluxes and small dimensions involved. However, the etching of large features (several microns or more), using currently available high-density plasma etchers, can exhibit a notching effect that extends laterally several microns. The extent of footing depends on many variables such as the electron temperature,[2–4] the ion energy,[5] the ion/electron current to the surface, the size of the feature and the amount of sidewall passivation.

In particular, the dependence of this effect on etching conditions in a time multiplexed deep etcher (TMDE) has been described elsewhere.[5] In this exercise we used a deep reactive ion etching (DRIE) tool from Surface Technology Systems.[6] This tool multiplexes between a passivating cycle that employs a C_4F_8 plasma and an etching cycle with a SF_6 plasma. In addition to the 13.65 MHz rf power applied to the electrodes, the tool has another rf power source connected to a single-turn coil around the processing chamber. This dual rf power arrangement permits the generation of high-density plasmas for deep silicon etching applications. A complete description of this piece of equipment as well as process optimization techniques can be found elsewhere.[7–9]

The notching effect also has a strong dependence on the aspect ratio of etched features, as can be seen in Fig. 2. Aspect ratio is the ratio of depth to horizontal opening for a particular trench. For aspect ratios of the order of 1 or less, there is enough electron bombardment at the lower part of etched structures, and on the bottom surface, to preclude the charge buildup associated with the footing effect. It can be further observed in the scanning electron microscopy (SEM) micrographs (a) and (b) in Fig. 2 that the notching is less than 1 μm deep. However, as the aspect ratio increases the footing depth also increases. It then achieves a depth of 1.84 μm for an aspect ratio of 1.95, Fig. 2(c), and even 5.63 μm when the aspect ratio reaches 3.30 in Fig. 2(d). As the aspect ratio increases even further, the footing depth decreases to 3.96 μm for an aspect ratio of 5.16 [see Fig. 2(e)], and 1.89 μm when the aspect ratio reaches 7.25 as can be seen in Fig. 2(f). For narrow trenches, there is a significant drop in the etching rate due to shadowing and the concomitant ion flux reduction reaching the bottom surface. The reduction in notching depth observed in Figs. 2(e) and 2(f) is then related to the reduced time the bottom surface is exposed to ion bombardment, and the decreased ion current at the bottom of a trench. The preceding observations suggest that notching can be controlled by tailoring the aspect ratio of etched trenches.

Another variable of interest that concerns notching is the amount of overetching time. The relevance of this variable is shown in Fig. 3, which includes an array of trenches similar to those of Fig. 2 but with an additional 10 min etching time. Footing remained small in those cases involving low aspect ratio trenches as can be seen in the micrographs (a) and (b) in Fig. 3. However, in all higher aspect ratio cases, and compared to similar trenches in Fig. 2, the notching effect became deeper and wider as shown in the micrographs (c) through (e) in Fig. 3.

The observations indicate that feature charging is the

[a]Electronic mail: ayon@mtl.mit.edu

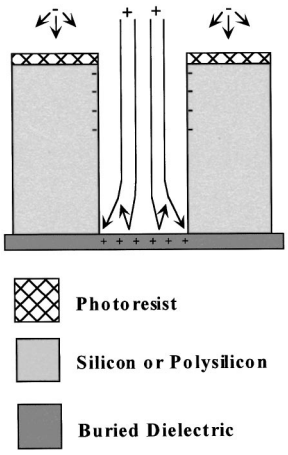

FIG. 1. Footing originates from the isotropic flux of electrons on the sidewalls of the feature that creates a negative charge near the feature opening. The flux of electrons to the lower sidewalls and bottom of the feature is limited by the reduced view factor to the plasma and the repulsive negative charging near the feature opening. The bottom regions of narrow spaces charge positively due to the greater monodirectional ion flux.

main mechanism for explaining the footing effect,[1–3,5] and that the charging potential of etched features on a wafer is influenced by their electrical connection.[4,10–12] Thus, for a given trench width, different notch depths can be expected across a wafer on features charging at different potentials. Similarly, notch symmetry can be predicted for features charging at the same potential. The micrograph shown in Fig. 4 is an example where both symmetric and asymmetric notches are observed on features with dissimilar electrical connections.

It is also relevant to ponder the influence of etching species availability on footing, considering that upon reaching the buried dielectric layer, the concentration of fluorine is expected to increase. It has been reported that conditions that promote the availability of fluorine or decrease the concentration of etching byproducts, such as higher chamber pressure settings or higher SF_6 flow rates, decrease[5] the extent of notching with respect to the overetching time. Furthermore, the excess supply of fluorine cannot explain the observed asymmetrical variations in notching shown in Fig. 4, or the absence of notch formation for trenches when low aspect ratios are involved (see Figs. 2 and 3), where etching species are predictably more abundant. Also, the shape of the notches appears to be line of sight with the deflection of the ions leaving the silicon dioxide near the interface, instead of being circular with the center based upon the sidewall. Thus, the observations suggest that surface charging controls footing, although the availability of etching species could have a synergistic effect in notch formation.

The footing or notching effect described in the previous paragraphs can be utilized for releasing silicon structures during processing of silicon-on-insulator (SOI) wafers. For these applications it is also necessary to emphasize the rel-

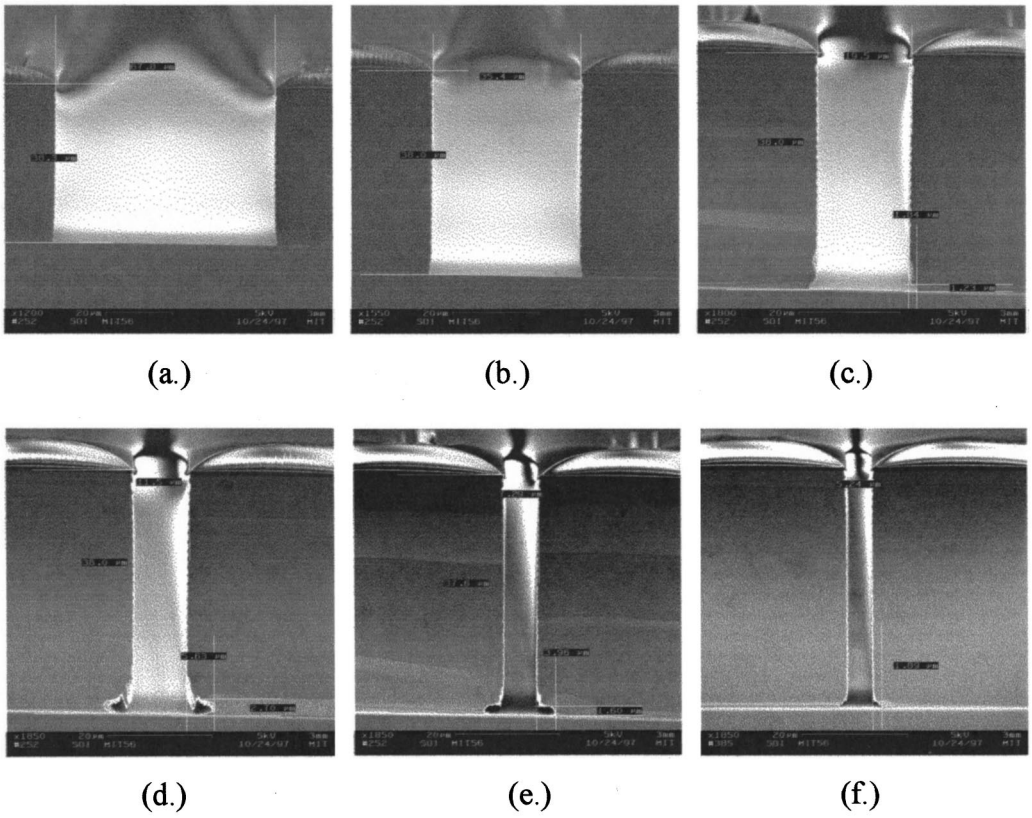

FIG. 2. Footing effect dependence on the aspect ratio of etched structures. Aspect ratio is defined as the ratio of depth to opening of a particular trench. Thus, the respective aspect ratios for the SEM micrographs shown are 0.56 in (a), 1.07 in (b), 1.95 in (c), 3.30 in (d), 5.16 in (e), and 7.25 in (f).

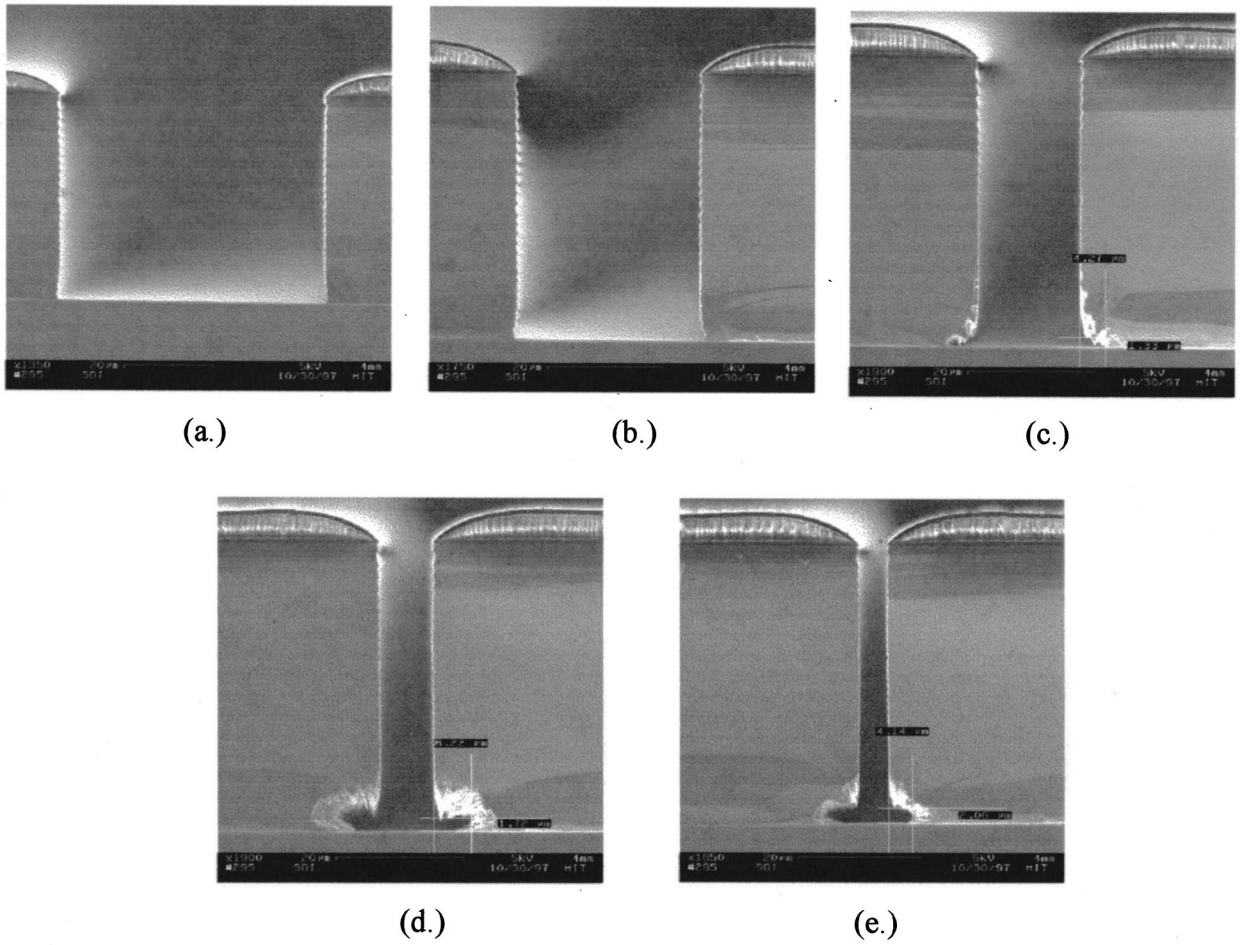

FIG. 3. Dependence of footing on overetching time. The SEM micrographs show trenches similar to those in Fig. 2, that have been etched 10 min more compared to those in Fig. 2.

evance of charging and ion bombardment during the microfabrication of cantilevered beams. In the case of a simple fluorinated, isotropic glow discharge, when releasing a silicon beam that has its sidewalls protected by a film such as silicon dioxide, the spontaneous etch of silicon causes the quick loss of the silicon in the beams,[13,14] leaving behind only the protective shell. By comparison, this deleterious effect is small when exploiting the footing effect. The explanation underlying this observation is that during the release of structures the tool is still operating in TMDE mode, therefore, protective films are also being deposited within the notch. Thus, ion bombardment is still required to proceed with the etch.

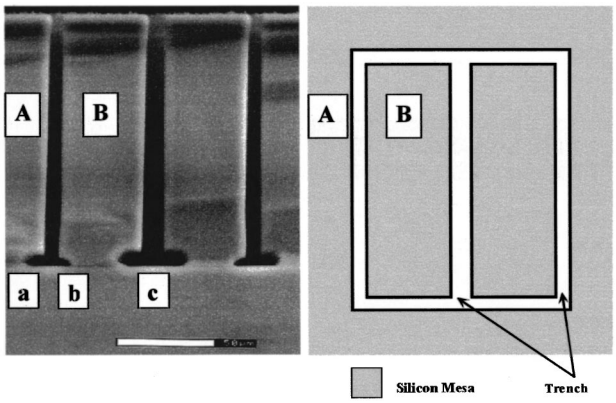

FIG. 4. Electrical connection between different etched features influences the extent of footing. Thus the different depths achieved by notches a and b can be explained in terms of differences in the charging potential of the respective features. Similarly, the observed symmetry in the notches identified with c is expected for features charging at the same potential.

II. ELECTROSTATIC ACTUATORS

The observed extent of footing can, therefore, be used to microfabricate high aspect ratio suspended structures for such applications as microvalves, micropumps, and microrelays. However, devices using electrostatic actuation also require electrical isolation to avoid failure by stiction. Several techniques have been proposed to solve this problem, usually involving additional film depositions such as silicon dioxide.[13,14]

The suggested approach contained in this article is the utilization of *in situ* deposited fluorocarbon films employing the same TMDE piece of equipment. It has been previously reported[15] that the characteristics of those fluorocarbon films

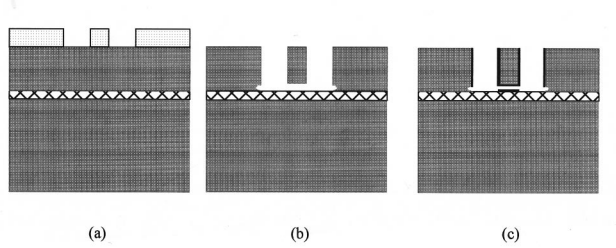

FIG. 5. Sequence for the microfabrication of released structures. After the photolithographic step (a), a TMDE tool can perform all the remaining steps *in situ*: silicon etch, (b) release of structures during overetch, ash photoresist, conformational deposition of a fluorocarbon film, and (c) use of an oxygen plasma to remove the fluorocarbon film from all horizontal surfaces.

have a strong dependence on deposition conditions, and that the deposition rate can exceed 0.18 μm/min. Therefore, the application of the footing effect in combination with the *in situ* deposition of electrical isolation films enables a new microfabrication sequence detailed in the following paragraphs.

Step (i). Transfer the topography to photoresist using a standard photolithography step. See Fig. 5(a).

Step (ii). Etch the silicon substrate until the underlying dielectric film is reached. Etching conditions and optimization of operating points during TMDE can be found elsewhere.[7,8] The TMDE processing conditions used in this exercise were as follows: during the passivating cycle 40 sccm of C_4F_8 were flown 11 s, with the electrode power set at 6 W and the coil power at 600 W; during the etching cycle 105 sccm of SF_6 were flown 14 s (with an additional overlap over the passivating cycle of 0.5 s) with the electrode power set at 12 W and the coil power set at 750 W. The position of the throttle valve was fixed at 65° during operation.

Step (iii). During the overetching time, charging produces the footing effect,[1] and the structures are released. This time can be tailored to release the widest feature in the design. As was previously mentioned, the deleterious effect of losing height control in narrower beam due to spontaneous silicon etching reported in other schemes is very small during this step.

Step (iv). Photoresist can be removed *in situ* with an oxygen glow discharge. See Fig. 5(b).

Step (v). Operating the equipment in continuous mode, and flowing only C_4F_8, a fluorocarbon film is deposited on all surfaces.

Step (vi). Additional *in situ* oxygen plasma will preferentially remove the passivation film from all horizontal surfaces exposed to ion bombardment, while preserving the film on sidewalls.[5] Auger spectroscopy was used to inspect the horizontal and vertical surfaces after exposure to oxygen plasma. Figure 5(c) shows the cross section of a completed device.

III. TESTING

An electrostatic actuator was built to validate the preceding approach. The design (see Fig. 6) included beams 3.8 μm wide, 1000 μm long etches using SOI wafers supplied by Motorola with a single crystal silicon ⟨100⟩ film 38 μm thick, and of 5–20 Ω cm resistivity. Upon transferring the topography to photoresist, the devices were prepared following the process outlined in Fig. 5. After photolithography, all necessary steps were performed in the same DRIE tool including silicon etching, structure release, photoresist ashing, fluorocarbon film deposition as well as its removal from all horizontal surfaces. After ashing the photoresist (step iv), the wafer were cleaved and half of each wafer was tested with-

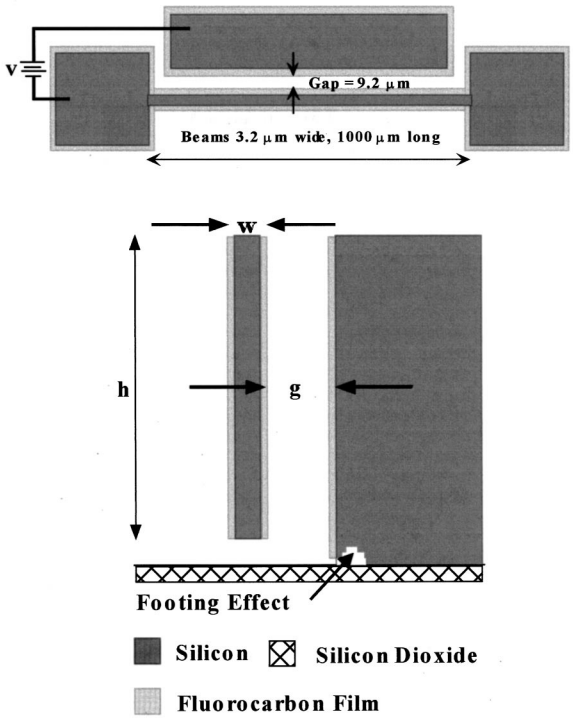

FIG. 6. Drawing of the electrostatic actuator described herein.

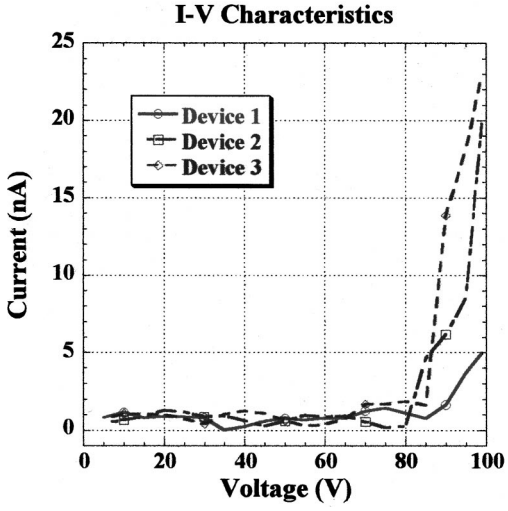

FIG. 7. *I–V* characteristics of the electrostatic actuator described in this article. Fluorocarbon films for electrical isolation purposes were deposited *in situ*.

out the additional fluorocarbon film deposited, while the other half continued with steps (v) and (vi) outlined in the previous paragraph.

Testing was done by applying a ramping voltage in steps of 5 V, between the points illustrated in Fig. 6. Although the pull-in voltage is of the order of 85 V, it was decided to apply up to 100 V to further stress the passivation film. Actuators without the additional passivating film failed by stiction within 50 pull-in cycles. Actuators that followed the sequence described herein (see Fig. 5), continued operating without failure or noticeable performance degradation after 10^5 pull-in cycles. Figure 7 shows the I–V characteristics for three typical devices obtained with a semiconductor parameter analyzer. Even though there is a noticeable increase in current drained beginning at pull-in voltage, the leakage current only increased from $\approx$1 nA to $<$25 nA even for an applied 100 V.

IV. CONCLUSIONS

We have, therefore, demonstrated the application of the footing effect in the microfabrication of suspended structures using a process compatible with SOI technology. The measured performance of the microfabricated electrostatic actuators demonstrates the usefulness of the *in situ* deposition of fluorocarbon films for electrical isolation purposes. Furthermore, after photolithography, all steps required to microfabricate suspended structures (i.e., silicon etching, release of devices, photoresist removal, deposition of electrical isolation films and clearing of fluorocarbon films from all horizontal surfaces) are done in the same high-density plasma, DRIE tool. This process is, therefore, compatible with a large variety of microelectromechanical systems (MEMS) applications.

ACKNOWLEDGMENTS

The U.S. Army Research Office, Dr. R. Paur, Technical Manager, and DARPA, Dr. R. Nowak, Program Manager, supported this project. One of the authors (R.A.B.) was supported by a NSF Fellowship. The cooperation of the staff of the Microsystems Technology Laboratories at MIT and the processing help of Kurt Broderick are also appreciated.

[1]J. C. Arnold and H. H. Sawin, J. Appl. Phys. **70**, 5314 (1991).
[2]S. Tabara, Jpn. J. Appl. Phys., Part 1 **35**, 2456 (1996).
[3]G. S. Hwang and K. P. Giapis, J. Vac. Sci. Technol. B **15**, 70 (1997).
[4]N. Fujiwara, T. Maruyama, and M. Yoneda, Jpn. J. Appl. Phys., Part 1 **34**, 2095 (1995).
[5]A. A. Ayón, K. Ishihara, R. A. Braff, H. H. Sawin, and M. A. Schmidt, 45th International Symposium of the American Vacuum Society, Baltimore, MD, 2–6 November 1998.
[6]Surface Technology Systems USA Inc., Redwood, CA.
[7]A. A. Ayón, C. C. Lin, R. Braff, R. Bayt, H. H. Sawin, and M. Schmidt, J. Electrochem. Soc. **146**, 339 (1999).
[8]A. A. Ayón, C. C. Lin, R. Braff, R. Bayt, H. H. Sawin, and M. Schmidt, 1998 Solid Sate Sensors and Actuator Workshop, Hilton Head, SC, 8–11 June 1998.
[9]J. Bhardwaj, H. Ashraf, and A. McQuarrie, Annual Meeting of the Electrochemical Society, Symposium on Microstructures and Microfabricated Systems, Montreal, Quebec, 4–9 May 1997, p. 118.
[10]T. Nozawa, T. Kinoshita, T. Nishizuka, A. Narai, T. Inoue, and A. Nakaue, Jpn. J. Appl. Phys., Part 1 **34**, 2107 (1995).
[11]T. Kinoshita, M. Hane, and J. P. McVittie, J. Vac. Sci. Technol. B **14**, 560 (1996).
[12]K. K. Chi, H. S. Shin, W. J. Yoo, C. O. Jung, Y. B. Koh, and M. Y. Lee, Jpn. J. Appl. Phys., Part 1 **35**, 2440 (1996).
[13]Z. L. Zhang and N. C. MacDonald, J. Micromech. Microeng. **2**, 31 (1992).
[14]A. A. Ayón, N. Kolias, and N. C. MacDonald, in Proceedings of the 1995 Asia-Pacific Microwave Conference, Taejon, South Korea, 10–13 October 1995, p. 147.
[15]A. A. Ayón, K. Ishihara, R. Braff, H. H. Sawin, and M. Schmidt, Fall Meeting of the materials Research Society, Boston, MA, 30 Nov.–4 Dec. 1998.